Applied Physics Letters

Formation of ultra-thin $Ge_{1-x}Sn_x$/$Ge_{1-x-y}Si_xSn_y$ quantum heterostructures and their electrical properties for realizing resonant tunneling diode

Cite as: Appl. Phys. Lett. **117**, 232104 (2020); https://doi.org/10.1063/5.0024905
Submitted: 12 August 2020 . Accepted: 12 November 2020 . Published Online: 08 December 2020

Galih Ramadana Suwito, Masahiro Fukuda, Edi Suprayoga, Masahiro Ohtsuka, Eddwi Hesky Hasdeo, Ahmad Ridwan Tresna Nugraha, Mitsuo Sakashita, Shigehisa Shibayama, and Osamu Nakatsuka

Applied Physics Letters ARTICLE scitation.org/journal/apl

Formation of ultra-thin $Ge_{1-x}Sn_x/Ge_{1-x-y}Si_xSn_y$ quantum heterostructures and their electrical properties for realizing resonant tunneling diode

Cite as: Appl. Phys. Lett. **117**, 232104 (2020); doi: 10.1063/5.0024905
Submitted: 12 August 2020 · Accepted: 12 November 2020 ·
Published Online: 8 December 2020

View Online Export Citation CrossMark

Galih Ramadana Suwito,[1] Masahiro Fukuda,[2] Edi Suprayoga,[3] Masahiro Ohtsuka,[2,4] Eddwi Hesky Hasdeo,[3,5] Ahmad Ridwan Tresna Nugraha,[3] Mitsuo Sakashita,[2] Shigehisa Shibayama,[2,a)] and Osamu Nakatsuka[2,6,a)]

AFFILIATIONS

[1]Department of Applied Physics, School of Engineering, Nagoya University, Furo-cho, Chikusa-ku, Nagoya 464-8603, Japan
[2]Department of Materials Physics, Graduate School of Engineering, Nagoya University, Furo-cho, Chikusa-ku, Nagoya 464-8603, Japan
[3]Research Center for Physics, Indonesian Institute of Sciences (LIPI), Tangerang Selatan 15314, Indonesia
[4]Advanced Measurement Technology Center, Institute of Materials and Systems for Sustainability, Nagoya University, Furo-cho, Chikusa-ku, Nagoya 464-8603, Japan
[5]Department of Physics and Materials Science, University of Luxembourg, L-1511 Luxembourg, Luxembourg
[6]Center for Integrated Research of Future Electronics, Institute of Materials and Systems for Sustainability, Nagoya University, Furo-cho, Chikusa-ku, Nagoya 464-8601, Japan

[a)]**Authors to whom correspondence should be addressed:** s-shibayama@nagoya-u.jp and nakatsuka@nagoya-u.jp

ABSTRACT

Huge thermal noise owing to the narrow energy bandgap is one of the critical issues for group IV-based photonics in the mid-infrared regime. With this motivation, we examined to form $Ge_{1-x}Sn_x/Ge_{1-x-y}Si_xSn_y$ quantum heterostructures (QHs) by molecular beam epitaxy for realizing resonant tunneling diodes composed of group-IV materials. We confirmed the formation of approximately 2 nm-thick $Ge_{1-x}Sn_x/Ge_{1-x-y}Si_xSn_y$ QHs with atomically flat interfaces by x-ray diffraction and transmission electron microscopy methods. Moreover, by the current density–voltage (J–V) measurement at 10 K, we observed the occurrence of a non-linear distinct hump in the J–V characteristic, which is possibly originated from quantum transport of heavy holes. According to the tunneling transmission spectra simulation result, the hump property would be due to two possible scenarios: a resonant tunneling of heavy holes in the QH and/or a resonance phenomenon that heavy holes pass just above a potential barrier.

Recently, $Ge_{1-x-y}Si_xSn_y$, which is an alloy of the group-IV semiconductors, Si, Ge, and semimetal Sn, has been an attractive material to realize scalable Si photonics, which are compatible with the current Si CMOS technology.[1] Moreover, the narrow bandgap nature of $Ge_{1-x}Sn_x$ makes it an ideal candidate material for group IV-based photonics in the mid-infrared (MIR) regime, which offers various potential applications from molecular spectroscopy[2] until MIR imaging.[3] Lasing[4–6] and photodetection[7] in the MIR regime have been experimentally demonstrated using $Ge_{1-x}Sn_x$, although the thermal noise due to its narrow bandgap is still one of critical issues. To suppress the thermal noise, it is important to develop devices with a functionality of negative differential resistance (NDR) such as resonant tunneling diodes (RTDs) based on $Ge_{1-x}Sn_x$ utilizing resonant tunneling transport.

Resonant tunneling is a quantum transport phenomenon of carriers (electrons or holes) manifested in a quantum heterostructure (QH) with two potential barriers. Because a quasi-bound energy state exists inside the quantum well, resonant tunneling occurs via this state when the energy of incoming carriers coincides with the quantized energy levels. As a result, NDR regions appear in its current– voltage characteristics.[8,9] We expect that $Ge_{1-x}Sn_x$-based RTDs will provide another degree of freedom for further development of

MIR technologies because the NDR of the RTD can provide electrical gain for optoelectronic devices, as has been demonstrated in conventional group-III–V compound semiconductors.[10–12]

Wu *et al.* have theoretically predicted that sandwiching $Ge_{0.9}Sn_{0.1}$ between moderate tensile-strained barrier layers of a $Ge_{1-x-y}Si_xSn_y$ ternary-alloy semiconductor will give the resonant tunneling due to sufficiently large band offsets.[13] However, the experimental proof of resonant tunneling for the $Ge_{1-x-y}Si_xSn_y/Ge_{1-x}Sn_x/Ge_{1-x-y}Si_xSn_y$ system has not yet been achieved, while an experimental evidence of band-to-band tunneling using $Ge_{1-x}Sn_x$ has been reported.[14] Recently, our group achieved $Ge_{1-x-y}Si_xSn_y/Ge_{0.9}Sn_{0.1}/Ge_{1-x-y}Si_xSn_y$ double heterostructures with a good crystallinity with the layer thickness of 15 nm each for various compositions of $Ge_{1-x-y}Si_xSn_y$ layers, which are targeted for laser applications.[15,16] We also experimentally confirmed that one of the $Ge_{1-x-y}Si_xSn_y/Ge_{0.9}Sn_{0.1}/Ge_{1-x-y}Si_xSn_y$ double heterostructures provides, in principle, sufficient band offsets for at least the first resonant tunneling state to occur.[16]

In this study, we demonstrated the formation of $Ge_{1-x}Sn_x/Ge_{1-x-y}Si_xSn_y$ QHs with an ultra-thin thickness of each layer and characterized their electrical properties. We first discuss the epitaxial growth of the QHs and their electrical transport properties by measuring the current–voltage characteristics. Then, we present theoretical simulation to understand the underlying quantum transport mechanism.

In this study, we prepared two different samples with different substrate types to clarify the carrier type for resonant tunneling. Both samples were designed to have the same energy band alignment with two potential barriers as shown in Fig. 1(a). The design of the band offset is followed from Ref. 15. We used *p*-type and *n*-type Ge(001) wafers as substrates for the epitaxial growth of $Ge_{1-x}Sn_x/Ge_{1-x-y}Si_xSn_y$ QHs of sample 1 and sample 2, respectively. After chemical cleaning of the substrates using de-ionized water, ammonia solution (NH_4OH: $H_2O = 1$: 4), and sulfuric acid (H_2SO_4: $H_2O = 1$: 7), in this order, the substrates were introduced into the ultra-high vacuum (UHV) chamber. Subsequently, the substrates were thermally cleaned at 430 °C in a UHV chamber with a pressure below 10^{-7} Pa for 30 min. After that, the epitaxial growth of $Ge_{1-x}Sn_x/Ge_{1-x-y}Si_xSn_y$ QHs was carried out with the molecular beam epitaxy (MBE) method at a base pressure below 10^{-7} Pa. Ge and Sn were deposited using Knudsen cells, and Si was deposited using electron beam evaporation. The QHs are composed of a 6 nm-thick quantum well (QW) structure [consisting of 2 nm-thick $Ge_{0.41}Si_{0.50}Sn_{0.09}$ (barrier), $Ge_{0.91}Sn_{0.09}$ (well), and $Ge_{0.41}Si_{0.50}Sn_{0.09}$ (barrier) layers] that is sandwiched between two 20-nm-thick $Ge_{0.96}Sn_{0.04}$ layers (spacers) as shown in Fig. 1(b). The growth temperature for the spacer and the barrier layers was 200 °C, and that of the high-Sn content well layers was 150 °C. According to previous studies,[17–19] the carriers in $Ge_{1-x}Sn_x$ and $Ge_{1-x-y}Si_xSn_y$ films without doping grown by MBE are likely to be *p*-type due to unintentional generation of holes related to vacancy defects. Finally, top and bottom Al electrodes were deposited using vacuum evaporation to characterize the electrical properties; top Al electrodes have a circular shape with an area of $1.2–2.2 \times 10^{-4}$ cm^2, whereas the bottom Al electrodes were deposited on the whole area of the wafer backside.

The epitaxial growth of each layer was examined during the MBE growth process using *in situ* reflection high-energy electron diffraction (RHEED) with the incident beam directed along the [1$\bar{1}$0] direction. The observed RHEED patterns of sample 1 after the growth of each layer are presented in Fig. 1(b). Streaky and spotty diffraction patterns are observed, indicating that the epitaxial layers with atomically flat surfaces were achieved. Next, the structural analysis was performed by x-ray diffraction two-dimensional reciprocal space mapping (XRD-2DRSM) with a monochromatic Cu Kα x-ray source

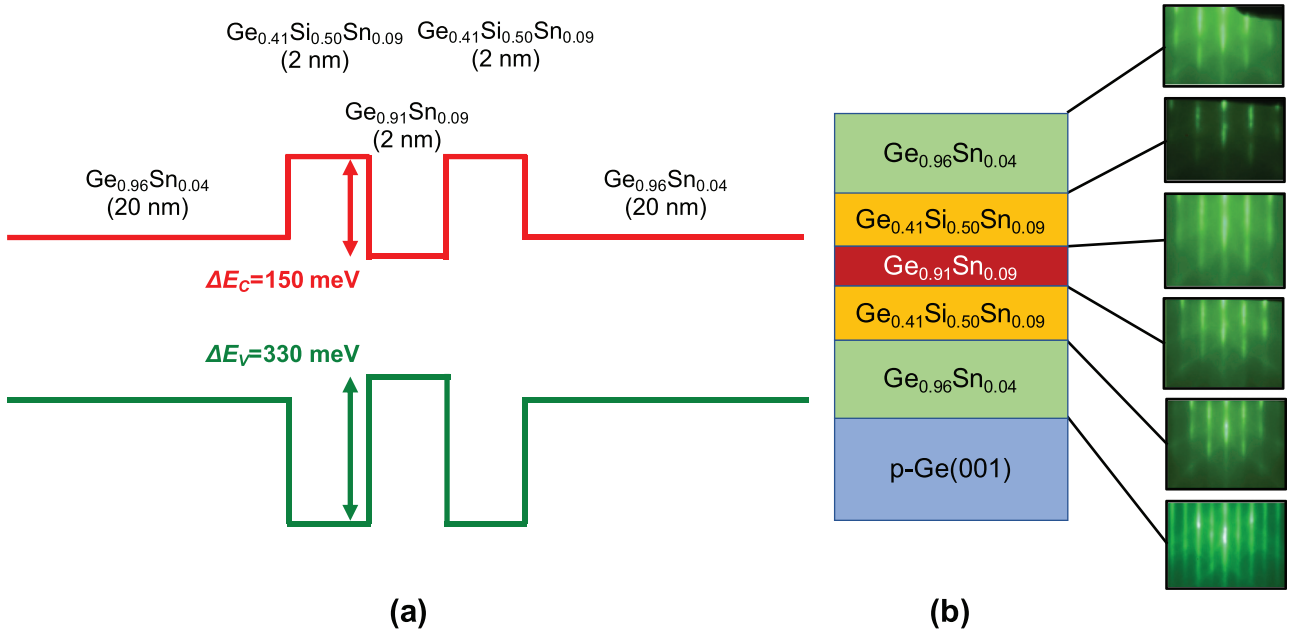

FIG. 1. (a) Schematic of the energy band alignment of the samples. (b) Schematic of sample 1 and the RHEED patterns after the growth of each layer.

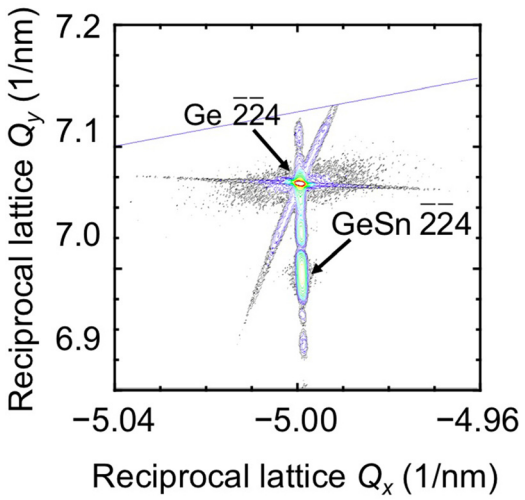

FIG. 2. XRD-2DRSM result around the reciprocal lattice point of Ge $\bar{2}\bar{2}4$.

(PANalytical MRD Pro). Figure 2 shows the XRD-2DRSM result of sample 1. The mapping result indicates the pseudomorphic growth of the $Ge_{1-x}Sn_x$ spacer layers without the formation of any strain-relaxed layers. By assuming Vegard's law, the Sn content in the $Ge_{1-x}Sn_x$ spacer layers was estimated to be 4–6%. Since it is difficult to judge whether or not the layer structures were grown only by XRD, we performed energy dispersive spectroscopy (EDS) elemental mapping using a scanning transmission electron microscope (STEM) JEM-2100F (JEOL, Japan) operating at 200 keV, equipped with an EDS silicon drift detector DrySD30GV (JEOL, Japan). Figure 3 shows the cross sectional STEM images of sample 1 and the corresponding relative concentration maps estimated from the STEM-EDS spectrum imaging data using Cliff–Lorimer k-factor implemented in Noran System Seven software (Thermo Fisher Scientific, USA). It can be observed that the 20 nm-thick spacer layers and the 6 nm-thick QW structure (composed of a 2 nm well and two 2 nm barrier layers) were sufficiently formed with flat interfaces, which is consistent with the RHEED results. It was also verified that the thickness fluctuation is less than 1 nm. In addition, Si only exists in the barrier layers as designed. Although the relative elemental contents in each QW layer can be quantitatively obtained from the STEM-EDS maps, their quantitative accuracy is relatively poor. This is due to the underestimation of the Si content as the fluorescent Si–K line was strongly absorbed within the specimen compared with Ge–K and Sn–L lines. Also, our present TEM specimen was too thick, and it showed a large thickness variation like a wedge-shaped specimen, indicating the accurate correction on x-ray absorption effect is difficult.[20] To obtain more accurate results, the STEM-EDS measurement using a flat thin specimen, and the content estimation by more accurate Cliff-Lorimer *k*-factors or ζ factors,[21] calibrated using appropriate reference specimens, are necessary in our future work.

From these structural analyses, it is concluded that the ultra-thin $Ge_{1-x}Sn_x/Ge_{1-x-y}Si_xSn_y$ QHs were formed, although the correct estimation of the element contents in QW layers is a remaining issue. Next, we discuss the electrical properties of ultra-thin $Ge_{1-x}Sn_x/Ge_{1-x-y}Si_xSn_y$ QHs.

The current density–voltage (*J*–*V*) characteristics of $Ge_{1-x}Sn_x/Ge_{1-x-y}Si_xSn_y$ QHs were measured at cryogenic temperatures using a Semiconductor Device Analyzer (Agilent, B1500A) to suppress strong influences of thermal-assisted scatterings at higher temperatures, such as from phonon scattering.[13] Figure 4 shows the *J*–*V* characteristics of sample 1 and sample 2 at 10 K. All samples exhibit non-linear *J*–*V* characteristics. For sample 1, a distinct hump property at a voltage around 0.3 V is observed although the NDR region is not clear. This property is more easily observed as a clear minimum in the differential conductance curve (Fig. 4, inset). We had also confirmed the reproducibility of this distinct hump property for other devices across the same wafer. This distinct hump property can be related to a huge leakage current in addition to a typical resonant tunneling NDR.[22] In our present sample, the huge leakage current can be attributed to the fact

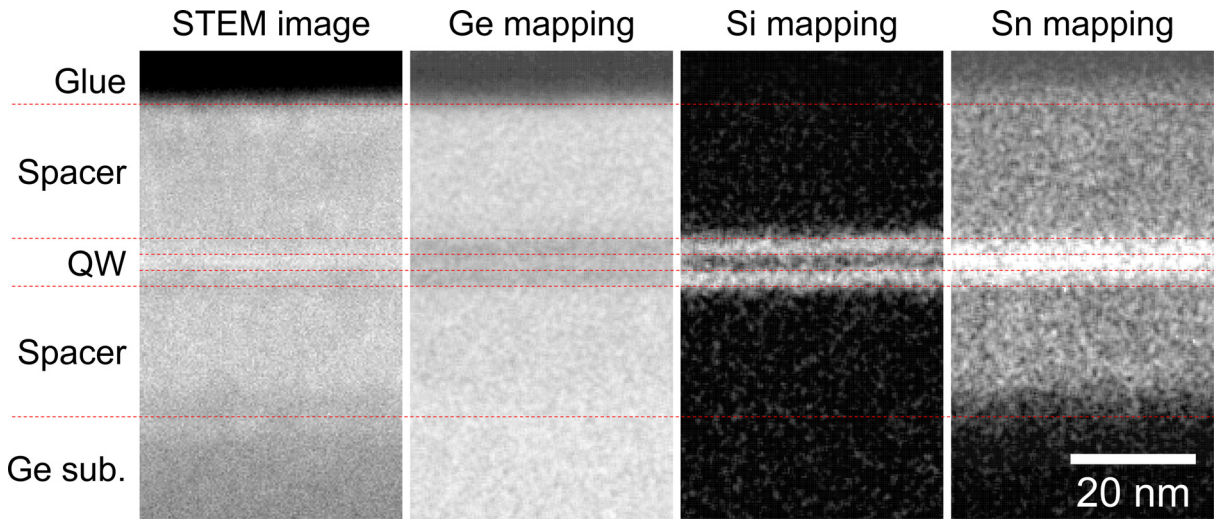

FIG. 3. Cross sectional STEM images with the EDS content mapping of sample 1.

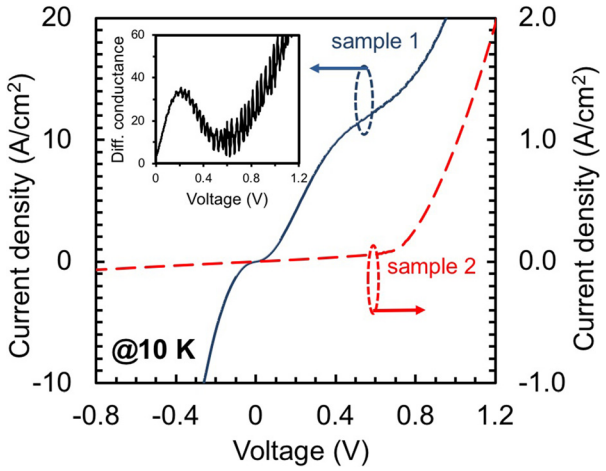

FIG. 4. *J–V* characteristics measured at 10 K of sample 1 (blue solid line) and sample 2 (red dashed line). Inset: the differential conductance curve of sample 1.

that the surface of samples prepared in this study was not passivated by either the insulator or mesa structure. Next, sample 2, which was grown on the *n*-Ge(001) substrate, shows a rectifying characteristic similar to that observed in a typical *p–n* junction despite the fact that the epitaxial layers were grown without doping. One plausible explanation for this characteristic is that the majority carriers of the epitaxial layers are holes, resulting in an unintentionally formed *p–n* junction in sample 2. Essentially, it suggests that the observed tunneling *J–V* hump in sample 1 should be related to the hole transport.

The hole tunneling transport observed in the present sample was also verified by simulating the transmission coefficient using the transfer matrix method.[23] The simulation was computed by matching the wave functions across the double potential barriers following the potential profile as shown in Fig. 5(a). In this simulation, the effects of band splitting of the light hole (LH) and the heavy hole (HH) valence bands were considered, as our samples are fully strained.[24] The fully strained HH valence band offset is expected to have a similar value to that of the relaxed case,[15] while the fully strained LH valence band offset is expected to have a much smaller value roughly half of the HH counterpart.[24] However, the exact values for the band offsets are not known at the present. Hence, in the simulation, we varied the valence band offset values to be 150–300 meV for HH. The choice of this offset range is based on our previous experiments reported in Ref. 15 expecting that the Si content in the barrier layers is between 23 and 50%. The valence band offset values for LH were assumed to be 75–150 meV, i.e., half of the HH case. In addition, the spacer and well layers were assumed to have the same band energy alignment, as shown in Fig. 5(a). We have verified that it is a fairly good assumption since changing the spacer layer valence band offset from 0 to 50 meV does not affect the general trend in the transmission spectra. In addition, the simulation assumed that the interferences come from perfectly coherent hole wave functions without any scatterings with LH and HH assumed to be distinguishable (no mixing)[25] and the effective mass assumed to equal to that of Ge, $0.044\,m_o$ and $0.284\,m_o$ for LH and HH, respectively.[26] Here, m_o is the rest mass of an electron (9.11×10^{-31} kg).

Figure 5(b) shows the simulation results for the case of HH. Two clear peaks can be observed in the tunneling transmission spectra of the HH with the lower energy peak well below the band offset. This essentially means that this lower energy peak corresponds to a resonant tunneling state. However, the higher energy peak exists at the energy beyond the band offset. It suggests that this higher energy peak is a result of a resonance phenomenon related to a normal quantum transport when holes pass just above a potential barrier. For the LH case, only one peak is observed at ~0.2 eV (i.e., beyond the band offset) with a very low peak-to-valley ratio. Considering these results and the fact that the HH has a larger density of states than the LH for fully strained $Ge_{1-x}Sn_x/Ge_{1-x-y}Si_xSn_y$ QHs,[24] the observed *J–V* humps are due to quantum transport of the HH.

In summary, we fabricated ultra-thin $Ge_{1-x}Sn_x/Ge_{1-x-y}Si_xSn_y$ QHs on Ge(001) substrates by MBE. The RHEED patterns reveal that the present QHs have relatively flat interfaces. Also, STEM-EDS and XRD analyses show the formation of QHs. In addition, from electrical characterization at cryogenic temperatures, we have experimentally observed a *J–V* tunneling hump in sample 1, which corresponds to quantum transport of holes. Considering the transmission spectra simulation showing the existence of a resonant tunneling state of HH and a resonance state related to a normal quantum transport when the HH passes just above a potential barrier, the observed hump property is due to the quantum transport of HH. The most essential next step is

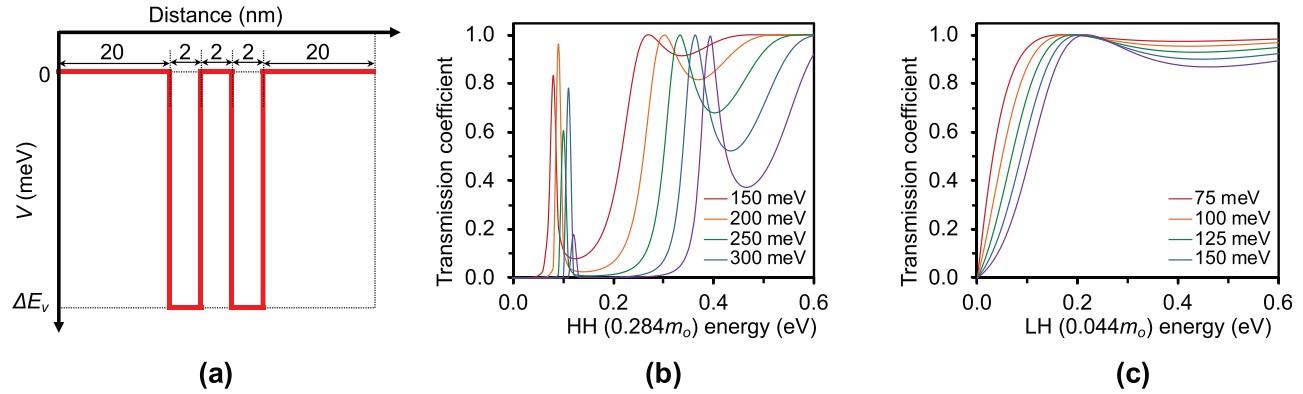

FIG. 5. (a) Potential profile used in the theoretical simulations. (b) Calculated transmission spectra for HH and (c) LH for various band offsets at equilibrium.

to clarify whether or not the observed hump property of the QHs is due to the resonant tunneling property of HH by developing a suitable passivation process to the current device structure using a mesa and/or oxide layer to suppress the huge leakage current. This work is an important step-up to pave the way for realizing practical RTDs using $Ge_{1-x}Sn_x/Ge_{1-x-y}Si_xSn_y$ QHs for further development of group IV-based MIR technology.

G.R.S. wishes to thank the Ministry of Education, Culture, Sports, Science, and Technology (MEXT) of Japan for the MEXT scholarship that he received during his study at Nagoya University. E.H.H. acknowledges support by the Luxembourg National Research Fund under Grants Nos. ATTRACT 7556175 and CORE 11352881.

DATA AVAILABILITY

The data that support the findings of this study are available from the corresponding author upon reasonable request.

REFERENCES

[1]R. Shoref, Nat. Photonics **4**, 495–497 (2010).
[2]J. Hodgkinson and R. P. Tatam, Meas. Sci. Technol. **24**, 012004 (2013).
[3]M. Razeghi and B.-M. Nguyen, Rep. Prog. Phys. **77**, 082401 (2014).
[4]S. Wirths, R. Geiger, N. V. D. Driesch, G. Mussler, T. Stoica, S. Mantl, Z. Ikonic, M. Luysberg, S. Chiussi, J.-M. Hartmann, H. Sigg, J. Faist, D. Buca, and D. Grützmacher, Nat. Photonics **9**, 88–92 (2015).
[5]D. Stange, N. V. D. Driesch, T. Zabel, F. A. Pilon, D. Rainko, B. Marzban, P. Zaumseil, J.-M. Hartmann, Z. Ikonic, G. Capellini, S. Mantl, H. Sigg, J. Witzens, D. Grützmacher, and D. Buca, ACS Photonics **5**, 4628 (2018).
[6]D. Rainko, Z. Ikonic, A. Elbaz, N. V. D. Driesch, D. Stange, E. Herth, P. Boucaud, M. E. Kurdi, D. Grützmacher, and D. Buca, Sci. Rep. **9**, 259 (2019).
[7]A. Gassenq, F. Gencarelli, J. V. Campenhout, Y. Shimura, R. Loo, G. Narcy, B. Vincent, and G. Roelkens, Opt. Express **20**, 27297 (2012).
[8]R. Tsu and L. Esaki, Appl. Phys. Lett. **22**, 562 (1973).
[9]L. L. Chang, L. Esaki, and R. Tsu, Appl. Phys. Lett. **24**, 593 (1974).
[10]T. J. Slight and C. N. Ironside, IEEE J. Quantum Electron. **43**, 580 (2007).
[11]B. Romeira, L. M. Pessoa, H. M. Salgado, C. N. Ironside, and J. M. L. Figueiredo, Sensors **13**, 9464–9482 (2013).
[12]S. Watson, W. Zhang, J. Tavares, J. Figueiredo, H. Cantu, J. Wang, E. Wasige, H. Salgado, L. Pessoa, and A. Kelly, Microwave Opt. Technol. Lett. **61**, 1121–1125 (2019).
[13]K.-Y. Wu, B.-H. Tsai, J.-Z. Chen, G.-E. Chang, V. I. Mashanov, H. H. Cheng, G. Sun, and R. A. Soref, IEEE Electron Device Lett. **34**, 951–953 (2013).
[14]C. S. Braucks, D. Stange, N. V. D. Driesch, S. Blaeser, Z. Ikonic, J. M. Hartmann, S. Mantl, and D. Buca, Appl. Phys. Lett. **107**, 042101 (2015).
[15]M. Fukuda, K. Watanabe, M. Sakashita, M. Kurosawa, O. Nakatsuka, and S. Zaima, Semicond. Sci. Technol. **32**, 104008 (2017).
[16]M. Fukuda, T. Yamaha, T. Asano, S. Fujinami, Y. Shimura, M. Kurosawa, O. Nakatsuka, and S. Zaima, Mater. Sci. Semicond. Process. **70**, 156–161 (2017).
[17]O. Nakatsuka, N. Tsutsui, Y. Shimura, S. Takeuchi, A. Sakai, and S. Zaima, Jpn. J. Appl. Phys., Part 1 **49**, 04DA10 (2010).
[18]S. Asaba, T. Yamaha, M. Kurosawa, M. Sakashita, N. Taoka, O. Nakatsuka, and S. Zaima, in Extended Abstracts of the 2013 International Conference on Solid State Devices and Materials, Fukuoka, Japan, 24–27 September (2013), pp. 1172–1173.
[19]T. Asano, N. Taoka, K. Hozaki, W. Takeuchi, M. Sakashita, O. Nakatsuka, and S. Zaima, Jpn. J. Appl. Phys., Part 1 **54**, 04DH15 (2015).
[20]H. Hoeft and P. Schwaab, X-ray Spectrom. **17**, 201 (1988).
[21]M. Watanabe and D. B. Williams, J. Microsc. **221**, 89 (2006).
[22]S. Bhattacharyya, S. J. Henley, E. Mendoza, L. G. Rojas, J. Allam, and S. R. P. Silva, Nat. Mater. **5**, 19–22 (2006).
[23]D. A. B. Miller, *Quantum Mechanics for Scientists and Engineers*, 1st ed. (Cambridge University Press, Cambridge, 2008).
[24]M. Fukuda, D. Rainko, M. Sakashita, M. Kurosawa, D. Buca, O. Nakatsuka, and S. Zaima, Semicond. Sci. Technol. **33**, 124018 (2018).
[25]J.-B. Xia, Phys. Rev. B **38**, 8365 (1988).
[26]O. Madelung, *Semiconductors: Data Handbook*, 3rd ed. (Springer, Berlin, 2003).